Activation Energy of Electron Transport in Dye-Sensitized TiO_2 Solar Cells

Gerrit Boschloo*,† and Anders Hagfeldt†

Department of Physical Chemistry, Uppsala University, P.O. Box 579, SE-751 23 Uppsala, Sweden

Received: March 16, 2005; In Final Form: April 25, 2005

Various characteristics of dye-sensitized nanostructured TiO_2 solar cells, such as electron transport and electron lifetime, were studied in detail using monochromatic illumination conditions. The electron transport was found to be a thermally activated process with activation energies in the range of 0.10−0.15 eV for light intensities that varied 2 orders of magnitude. Electron lifetimes were determined using a new method and found to be significantly larger (>1 s) than previously determined. An average potential was determined for electrons in the nanostructured TiO_2 under illumination in short-circuit conditions. This potential is about 0.2 V lower than the open-circuit potential at the same light intensity. The electron transport time varies exponentially with the internal potential at short-circuit conditions, indicating that the gradient in the electrochemical potential is the driving force for electron transport in the nanostructured TiO_2 film. The applicability of the conventionally used trapping/detrapping model is critically analyzed. Although experimental results can be fitted using a trapping/detrapping model with an exponential distribution of traps, the distribution parameters differ significantly between different types of experiment. Furthermore, the experimental activation energies for electron transport are smaller than those expected in a trapping/detrapping model.

Introduction

Solar cells based on the dye-sensitization of porous films of nanocrystalline TiO_2 have received much attention in recent years, due to their potential as low-cost photovoltaics and their interesting working mechanism that differs from conventional solar cells, resembling more natural photosynthesis.[1−3] The transport of electrons in dye-sensitized solar cells based on nanostructured TiO_2 is a relatively slow process.[4−15] Under full sunlight conditions, injected electrons travel on average for about 1 ms through the nanostructured TiO_2 film (∼10 μm thick) before reaching the conducting glass substrate. This transport time increases significantly at lower light intensities.[4−13] For an efficient solar cell, it is essential that the transport time is significantly shorter than the electron lifetime, which is the average time for recombination of an electron in TiO_2 with species in the electrolyte or adsorbed at the TiO_2. The electron lifetime also increases at lower light intensities.[7,10,12,16,17] The efficiency for charge collection is nearly independent of light intensity, as follows from the generally observed linear dependence of the short-circuit photocurrent on the light intensity.

It is generally accepted that the electron transport in nanostructured TiO_2 films occurs by diffusion.[2,3,18,19] No significant macroscopic electric fields can exist in the mesoporous structure as the undoped TiO_2 nanocrystals are surrounded by a concentrated electrolyte. The diffusion coefficients for electrons in nanostructured TiO_2 electrodes (in contact with electrolyte) are in the order of 10^{-8} to 10^{-4} cm^2 s^{-1}, strongly depending on the light intensity and electron concentration.[9−13,20] These values are orders of magnitude lower than that obtained for the TiO_2 (anatase) single crystal (∼0.5 cm^2 s^{-1}).[21] These observations can be explained by assuming that the electron transport in the nanostructured TiO_2 is dominated by multiple trapping/detrapping events.[5,8−10,15,22] A good fit to experimental data can be obtained if the density of traps in the band gap increases exponentially toward the conduction band.[8−10,15]

To verify the trapping/detrapping model, we have determined the activation energy for electron transport in dye-sensitized nanostructured TiO_2 solar cells. Surprisingly, there have been only a few investigations on the temperature dependence of the properties of nanostructured TiO_2. Greijer-Agrell et al. studied the temperature dependence of the conductivity and mobility of electrons in nanostructured TiO_2 immersed in an inert electrolyte.[20] The activation energy for the mobility ranged from 0 to 0.3 eV, depending on applied potential and electrolyte composition. Goossens et al. mentioned that the activation energy for electron transport in a dye-sensitized solar cell was 0.13 eV under 1/10 of a sun illumination, while it was negligible at full sunlight.[14] In this study, we have found activation energies for electron transport of 0.10−0.15 eV, depending on light intensity. Additionally, we have determined exponential trap distribution functions from transport and potential−charge measurements. The findings appear to be in conflict with existing trapping/detrapping models.

Experimental Procedures

Nanostructured TiO_2 films (thickness 12 μm) were deposited on conducting SnO_2:F coated glass (TEC 8, Pilkington) using a compression technique,[23] followed by heating to 450 °C for 0.5 h in air. The TiO_2 nanocrystal size was approximately 25 nm (Degussa P25). The films were sensitized overnight in an ethanol solution of 0.5 mM $(TBA)_2$ *cis*-$Ru(Hdcbpy)_2(NCS)_2$ dye (Solaronix), assembled with a platinized conducting glass counter electrode using a Surlyn frame, filled with the electrolyte (0.5 M LiI, 0.05 M I_2, and 0.5 M 4-*t* butylpyridine in 3-methoxypropionitrile) through a hole in the counter electrode, and sealed. The active area of the resulting solar cells was 0.785 cm^2 and the power conversion efficiency about 4−5%. All presented measurements are from a single solar cell; other cells gave very similar results. Illumination was from the dyed TiO_2 electrode side in all experiments.

Intensity-modulated photocurrent spectroscopy (IMPS) and transient measurements were performed in a darkened cabinet

* Corresponding author. Phone: +46 8 790 8178; fax: +46 8 790 8207; e-mail: gerrit@kth.se.

† Present address: Department of Chemistry, Physical Chemistry, Royal Institute of Technology, SE-100 44 Stockholm, Sweden.

10.1021/jp0513770 CCC: $30.25
Published on Web 05/26/2005

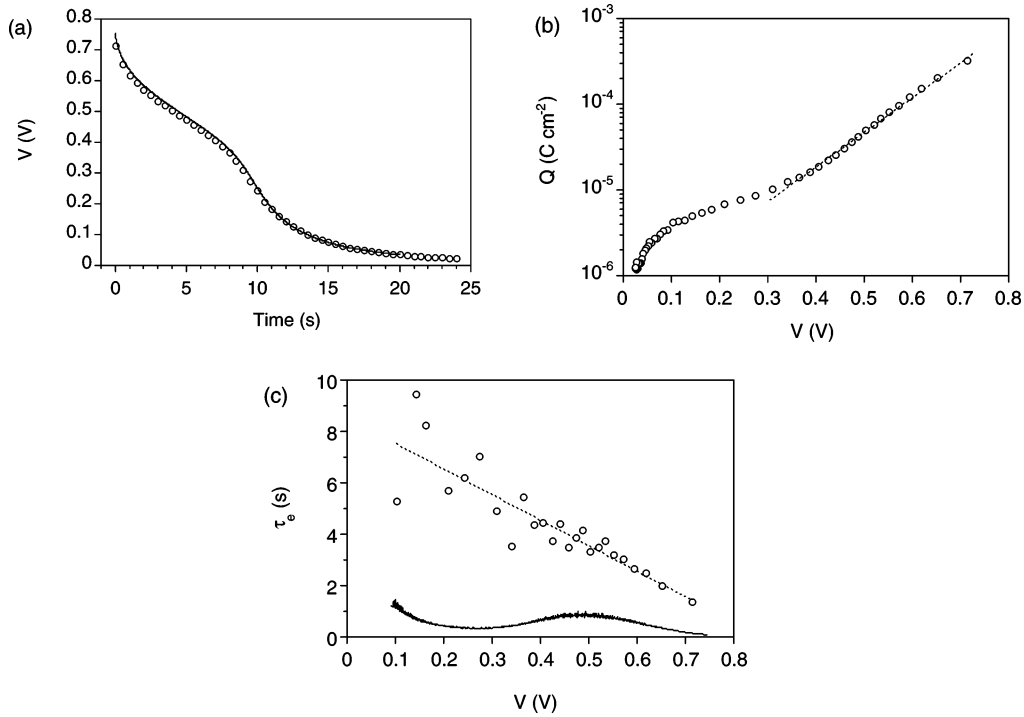

Figure 1. (a) Voltage decay transient of a nanostructured dye-sensitized solar cell after 5 s of illumination. Charge extraction measurements were done at the indicated points. (b) Extracted charge as function of the potential. The dotted line is an exponential fit for $V > 0.36$ V. (c) Electron lifetime as function of potential of the nanostructured TiO_2 film. Circles: τ_e determined from charge extraction measurements as function of time (eq 1). The dotted line is a guide to the eye. Drawn line: τ_e calculated from voltage decay transient (eq 4).

using a diode laser (635 nm, Coherent Lablaser) as the light source. For intensity-modulated photocurrent spectroscopy (IMPS), a sinus modulation with an intensity of about 1% of the total light output was added. The modulated photocurrent was measured by connecting the solar cell to a lock-in amplifier (Stanford Research Systems SR830) via a current amplifier (Stanford Research Systems SR570). Time constants were obtained using a nonlinear least-squares fitting procedure. A peltier element was used to control the temperature of the solar cell in the temperature-dependent studies. Photocurrent and voltage transients were recorded on a 16-bit resolution data acquisition board (National Instruments). Current decay transients were integrated numerically to obtain the accumulated charge in the mesoporous film. The charge recorded in the absence of laser excitation was subtracted to correct for any offset of the instrument.

Results

The relation between potential and charge in the dye-sensitized nanostructured TiO_2 solar cells was investigated using a voltage decay−charge extraction method, similar to that developed by Duffy et al.[24,25] Briefly, the solar cell was illuminated for 5 s under open-circuit conditions. Then, the voltage was left to decay for a certain period, t_d, in the dark. Finally, the cell was short-circuited, and the extracted charge (Q) was measured. Figure 1a shows the decay of the voltage after the laser was switched off. A charge extraction measurement was done at every indicated point. The drawn line is the voltage decay transient without charge extraction. The potential−charge curve is shown in Figure 1b. At potentials higher than 0.36 V, an exponential increase of the charge with potential is found. By combining the charge extraction data with the time delay, the lifetime of the electron (τ_e) can be calculated when a (pseudo) first-order recombination reaction is assumed

$$\tau_e = Q(t)\left(\frac{dQ(t)}{dt}\right)^{-1} \quad (1)$$

Figure 1c shows the lifetime of the electrons as a function of the potential of the dye-sensitized solar cell. The lifetime is very long, more than one second, and it increases gradually toward lower potentials.

A new technique was developed to obtain insight in the electrochemical potential of electrons inside the dye-sensitized nanostructured TiO_2 film when the solar cell is illuminated under short-circuit conditions. First, the solar cell was illuminated under short-circuit conditions. Then, the laser is switched off, and the cell is switched to open circuit simultaneously, while the voltage is monitored. Typical results are shown in Figure 2a. The voltage rises with a speed that is determined by the prior illumination intensity and reaches a maximum after a certain time, t_{max}. Thereafter, the voltage slowly decays to zero. The maximum voltage that is reached, hereafter referred to as the short-circuit voltage (V_{SC}), is related to the charge that is left in the nanostructured TiO_2. The measured V_{SC} and corresponding Q_{SC} values lie on the potential−charge curve of Figure 1b. V_{SC} gives an indication of the position of the quasi-Fermi level inside the nanostructured TiO_2 film. Figure 2b shows V_{SC} and V_{OC} as function of light intensity. The difference between V_{SC} and V_{OC} is almost constant (~0.22 V) at all light intensities studied. Figure 2c shows t_{max} as a function of V_{SC}. As t_{max} corresponds to the time required to obtain a uniform distribution of the electrons in the film (assuming that recombination occurs uniformly in the film), it can be considered as a transport time. The relation between t_{max} and V_{SC} appears to be exponential.

The transport of electrons in the dye-sensitized TiO_2 solar cell was studied using intensity-modulated photocurrent spectroscopy (IMPS). A single time constant (τ_{IMPS}) was extracted from the data taken in the frequency range of 0.5−1000 Hz. This time constant corresponds to the average time required for the electrons to reach the conducting glass substrate from

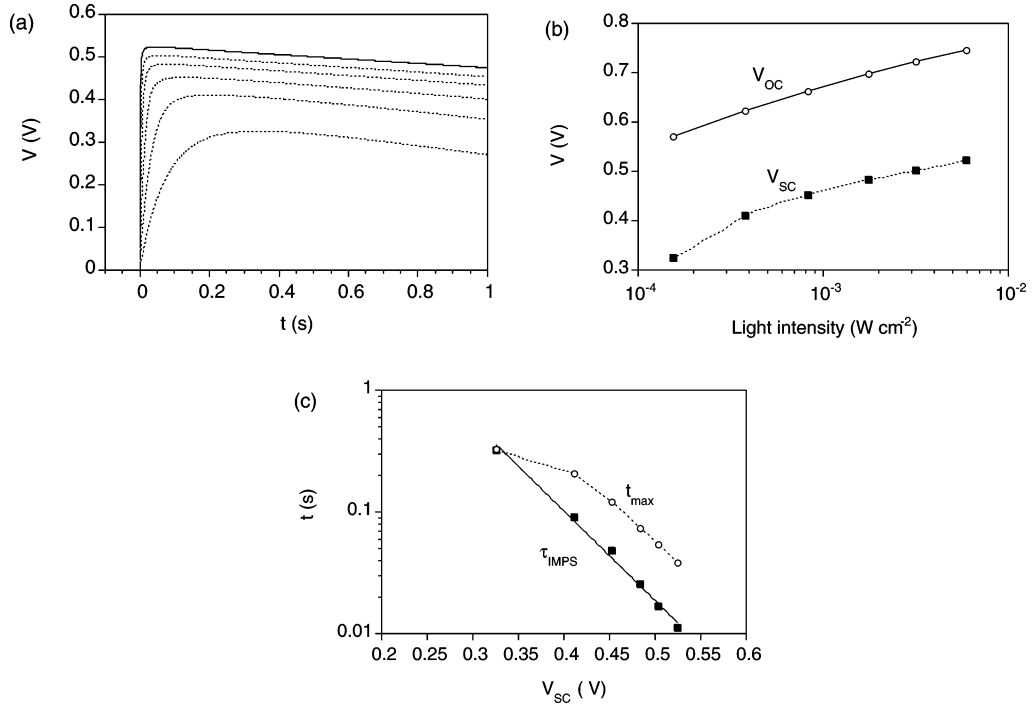

Figure 2. (a) Voltage transients of a nanostructured dye-sensitized solar cell recorded in the dark at open circuit, after illumination under short-circuit conditions. (b) Voltage maximum from (a), V_{SC}, as function of light intensity during the illumination period, and V_{OC} under steady-state illumination. (c) Relation between the time when voltage in panel (a) reaches its maximum (t_{max}, circles) and V_{SC}. Also, the transport time under continuous illumination (τ_{IMPS}, squares) is shown, where the drawn line is an exponential fit: $\tau_{IMPS} = 89 \exp(-16.9V_{SC})$, $R^2 = 0.997$.

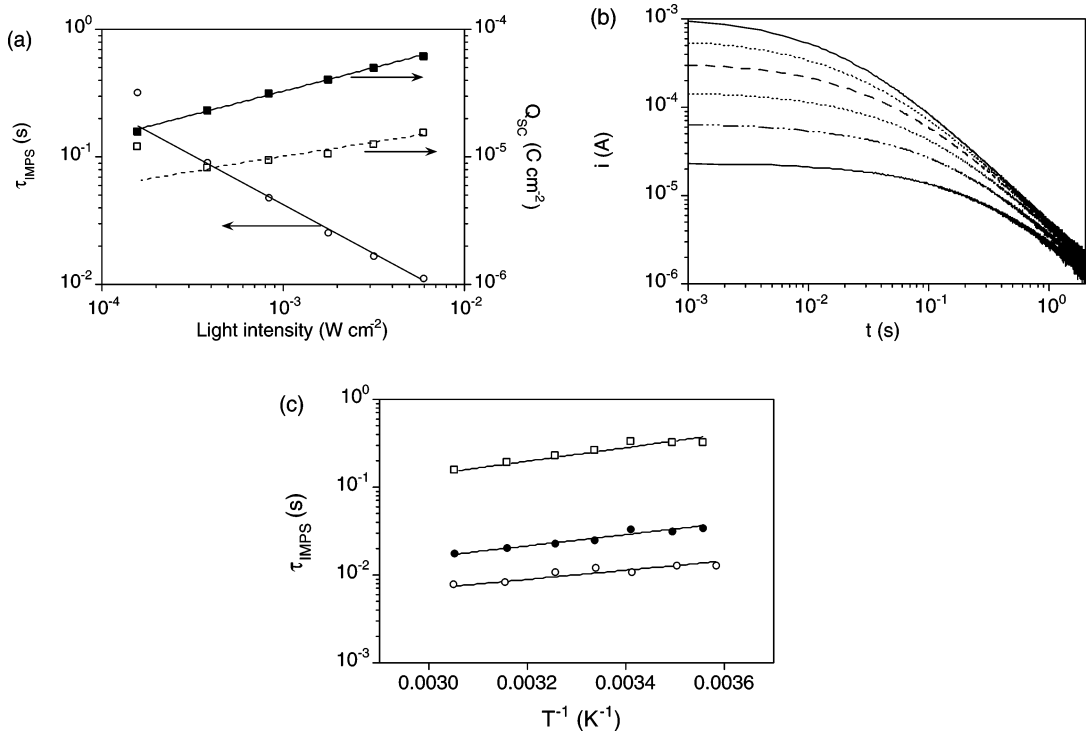

Figure 3. (a) IMPS time constant and extracted short-circuit charge (Q_{SC}) as function of light intensity. τ_{IMPS} is circles, Q_{SC} is filled squares, and the product of J_{SC} and τ_{IMPS} are empty squares. Exponents of the power-law fits are −0.77 (IMPS), 0.37 (Q_{SC}), and 0.23 ($J_{SC}\tau_{IMPS}$). The lowest intensity measurement was discarded in the fit of IMPS and $J_{SC}\tau_{IMPS}$. (b) Photocurrent decay transients with varying initial light intensities. (c) Temperature dependence of the electron transport (τ_{IMPS}) in a dye-sensitized nanostructured TiO_2 solar cell. The calculated activation energies are shown in Table 1.

the location where they are photogenerated. It is noted that recombination may affect the measured τ_{IMPS}. In the studied solar cells, however, the electron lifetime was very long. It is therefore reasonable to consider τ_{IMPS} as the transport time. Figure 3a shows the light intensity dependence of τ_{IMPS}. The transport time was about 10 ms at the highest light intensity. As has been observed in other studies, τ_{IMPS} follows a power-law dependence on the light intensity. The exponent was −0.77. In the same figure also the electronic charge in the nanostructured TiO_2 film under short-circuit conditions (Q_{SC}) is shown. Q_{SC} increases with the light intensity, following a power-law dependence with an exponent of 0.37. An interesting finding

TABLE 1: Characteristics of a Dye-Sensitized Nanostructured TiO_2 Solar Cell under Short-Circuit Conditions[a]

light intensity (mW cm^{-2})[b]	J_{SC} (A cm^{-2})	Q_{SC} (μC cm^{-2})	electrons/ particle[c]	V_{SC} (V)	τ_{IMPS} (ms)	$E_a(\tau_{IMPS})$ (eV)
5.89	1.39×10^{-3}	61.7	5.4	0.52	11.5	0.10 ± 0.02
1.76	4.15×10^{-4}	40.6	3.6	0.48	29.4	0.13 ± 0.02
0.156	3.72×10^{-5}	15.9	1.4	0.33	288	0.15 ± 0.03

[a] The activation energy for electron transport was measured in the range of 5−55 °C; other properties are measured at 20 °C. [b] Monochromatic light, $\lambda = 635$ nm. [c] The 12 μm thick film contains about 7.1×10^{13} TiO_2 particles cm^{-2}.

is that there is a clear relation between τ_{IMPS} and V_{SC} as can be observed in Figure 2c. This can be explained by the fact that the electrochemical potential, which is composed of electrostatic and chemical (concentration difference) contributions, is the driving force for electron transport. The electron transport time under short-circuit conditions decreases exponentially with increasing V_{SC}.

The charge in the nanostructured TiO_2 film under short-circuit conditions was determined using a current extraction method: the diode laser was switched off, and the following current decay transient was measured and integrated during a period of 10 s. As the electron lifetimes are long (>1 s, see Figure 1c), nearly all the charge will be extracted. Typical current decay transients are shown in Figure 3b in a double logarithmic plot. It is interesting to note that the slope of the transients is close to −1 at longer times.

Figure 3c shows the temperature dependence of the electron transport in the solar cell in the range of 5−55 °C at three different light intensities. τ_{IMPS} decreases with increasing temperature, indicating that the electron transport is a thermally activated process. Using the Arrhenius equation, activation energies ranging from 0.10 to 0.15 eV were determined from the slopes in Figure 3. The results are summarized in Table 1. The activation energies have a weak dependence on the light intensity: smaller activation energies are found at higher monochromatic light intensities. The activation energies determined here are similar to those found by Goossens et al. under low illumination intensity.[14] They observed, however, no activation energy under full sunlight. In an additional experiment, we found an activation energy of about 0.1 eV even under conditions approaching full sunlight ($J_{SC} = 5$ mA cm^{-2}). We did, however, use only monochromatic light (635 nm) in contrast to Goossens' study, where white light from a halogen lamp was used. The infrared part of this light may have interfered with the measurement, as (trapped) electrons in TiO_2 can absorb this light.

Discussion

Potential−Charge Relation and Electron Lifetime.

The relation between the open-circuit potential (V_{OC}) and the density of conduction band electrons in the nanostructured semiconductor is given by[26]

$$V_{OC} = \frac{kT}{e}\ln\left(\frac{n}{n_0}\right) \tag{2}$$

where kT is the thermal energy, e is the quantum charge, and n and n_0 are the concentration of conduction band electrons under illumination and in the dark, respectively. In accordance to eq 2, the charge increases exponentially with the measured V_{OC}, at least at potentials larger than 0.36 V (see Figure 1b). The exponent is, however, much smaller than $(e/kT)V_{OC}$ that follows from eq 2. Similar observations have been done in other investigations.[25,27] The observed exponential increase of charge versus potential can be explained by assuming an exponential distribution of traps below the conduction band edge. Such a trap distribution can be described by[8−10]

$$N_T(E) = N_{T0}\exp\left(\frac{E - E_{F0}}{m}\right) \tag{3}$$

where N_{T0} is the trap state density at E_{F0}, which is the Fermi-level of the TiO_2 in the dark, and m is the slope of the trap distribution. Using this approach, m is determined to be 105 meV for $V > 0.36$ V. It is noted that part of the extracted charge is not stored in the TiO_2 particles but resides at the SnO_2:F/electrolyte interface. This is a rather small effect, and we have not made corrections for it in this study.

The electron lifetimes derived from the voltage decay−charge extraction method are very long, more than 1 s. This long lifetime ensures that practically all injected electrons will be collected at the conducting glass substrate. It should be noted, however, that the measured lifetime only refers to the reaction of electrons with triiodide in the redox electrolyte in the dark. Under illumination, there are additional recombination pathways, as electrons can also react with oxidized dye molecules and $I_2^{-\bullet}$ radicals that are formed as an intermediate in the regeneration of the dye.[28,29] Preliminary experiments in our laboratory suggest that τ_e under illumination can be about 2 times smaller than in the dark. Recently, Zaban et al. proposed the use of simple potential decay measurements to determine the electron lifetime in nanostructured dye-sensitized solar cells.[26,30] If eq 2 is valid, than the electron lifetime follows directly from the slope of the voltage decay curve according to eq 4

$$\tau_e = -\frac{kT}{e}\left(\frac{dV_{OC}}{dt}\right)^{-1} \tag{4}$$

This relation also holds when a trap distribution such as eq 3 is present. In that case, τ_e represents the average lifetime of both trapped and free electrons. The resulting lifetimes of this approach are also shown in Figure 1c. Much smaller electron lifetimes are found using this method as compared to the voltage decay−charge extraction method. In the latter method, no assumptions regarding the relation between charge and potential need to be done. The electron lifetime follows directly from the measured charge differences. Therefore, we propose this method to be more reliable. The large difference as compared to lifetimes obtained from the voltage decay method (eq 4) suggests that the generally accepted relation between charge and potential in mesoporous nanocrystalline semiconductors (eq 2) is not valid.

A certain electrochemical potential will develop in the dye-sensitized nanostructured TiO_2 film when it is illuminated under short-circuit conditions. The short circuit (light)/open circuit (dark) switching experiment described in the Results (Figure 2) gives a good indication of the magnitude of this potential. Considering that the potential varies along the thickness of the film, being zero at the substrate side, one can expect the maximum potential to be slightly higher than the measured V_{SC}. As stated earlier, V_{SC} corresponds approximately to the position of the quasi-Fermi level inside the nanostructured TiO_2 under illumination and under short-circuit conditions. The energy of the conduction band edge (E_C) of TiO_2 is estimated to be located at about 0.8 eV versus E_{F0}. From the results shown in Figure 2, it follows that ($E_C - E_F$) varies from about 0.28 eV for the highest light intensity to 0.47 eV for the lowest light intensity studied.

TABLE 2: Parameters of the Trapping/Detrapping Model with Exponential Trap Distribution[a] Obtained for the Nanostructured Dye-Sensitized Solar Cell using Various Experimental Techniques

experiment	m (meV)	N_{tot} (cm^{-3})[b]
Q_{SC}−light intensity	69	1.6×10^{20} (1400)
τ_{IMPS}−light intensity	112	
V−Q	105	8.7×10^{18} (73)

[a] See eq 3. [b] Total density of traps in the TiO_2 band gap, assuming $E_C = 0.8$ eV vs E_{F0} and $N_C = 10^{20}$ cm^{-3}. The number of traps per TiO_2 particle is shown in parentheses.

In a trapping/detrapping model, these values would correspond to the effective trap depth at the respective light intensities.

The composition of the electrolyte (concentration, nature of the cations, additives) has marked effects on the electron lifetime and the electrochemical potential in the TiO_2, as well as on the electron transport. We will address this topic in a forthcoming publication.

Electron Transport and Accumulation.

The electron transport time in nanostructured TiO_2 films varies with light intensity and accumulated electron charge (see Figure 3). Under full sunlight illumination and short-circuit conditions (photocurrent density, ~15 mA cm^{-2}), we estimate by extrapolation of the data in Figure 3a that the transport time will be about 2 ms and the average charge about 13 electrons per TiO_2 particle. The number of electrons per particle determined here is much higher than in previous studies that used either IMPS,[14] IMVS (intensity-modulated photovoltage spectroscopy),[16] or photoinduced absorption experiments.[17] This difference can be attributed to the larger TiO_2 particle size used in this study.

From Figure 2c, it can be derived that the electron transport time varies exponentially with V_{SC}. A certain relation between V_{SC} and τ_{IMPS} can be expected as the gradient in the electrochemical potential is responsible for the electron transport in the nanostructured TiO_2 film. Extrapolation of V_{SC} to 0 V gives a transport time of about 90 s. Under such conditions, corresponding to a situation without illumination, there is no gradient in electron concentration in the film. Considering that the electron movement is a random walk and that the electron reaches the conducting substrate in about 90 s, we can estimate that the electron diffusion coefficient in the direction perpendicular to the substrate is about 2×10^{-9} cm^2 s^{-1}. The electron jumps from one TiO_2 particle to the next in about 10^{-3} s in this direction.

The variation of Q_{SC} and τ_{IMPS} with light intensity can be explained using the trapping/detrapping model with exponential trap distribution. The trap distribution parameter m (see eq 3) follows directly from the slopes of the double logarithmic plots of Q_{SC} and τ_{IMPS} versus light intensity. The slope is kT/m and $(kT/m - 1)$ for Q_{SC} and τ_{IMPS}, respectively.[8] The resulting m-values are shown in Table 2. There is a good correspondence in m-values from the potential−charge and τ_{IMPS}-light intensity measurements ($m = 110$ meV), but a clearly different value is found in the Q_{SC} versus intensity measurement ($m = 69$ meV). Furthermore, there is 1 order of magnitude difference in the estimated total trap densities. It is also noted that the determined Q_{SC} values are much larger than the product of J_{SC} and τ_{IMPS} that was used to estimate Q_{SC} by van de Lagemaat and Frank[8] (see Figure 2a). The experimentally determined electron concentration in nanostructured TiO_2 is thus significantly larger than the predicted values from the trapping/detrapping model with exponential trap distribution, calculated from the experimental short-circuit current and IMPS data.

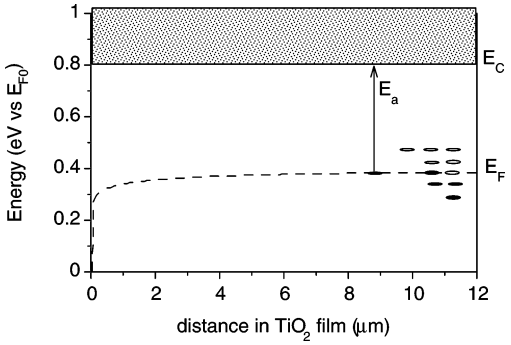

Figure 4. Calculated Fermi-level profile in the nanostructured TiO_2 film for the trapping/detrapping model with exponential trap distribution, using eqs 3 and 5. Some trap levels are indicated at the right-hand side. The parameters used are $E_C = 0.8$ eV vs E_{F0}, $N_C = 10^{20}$ cm^{-3}, $D_C = 0.5$ cm^2 s^{-1}, photon flux $= 1.89 \times 10^{16}$ cm^{-2} s^{-1}, $m = 69$ meV, $\alpha = 5.2 \times 10^4$ m^{-1}, and $N_{T0} = 2.2 \times 10^{16}$ cm^{-3} eV^{-1}. The last two parameters are chosen to fit the highest light intensity case in Table 1 with respect to J_{SC} and Q_{SC}, respectively.

The electron transport in nanostructured TiO_2 is a thermally activated process with activation energies in the range of 0.1−0.15 eV. Within a trapping/detrapping model, this would imply that the effective trap depth is 0.1−0.15 eV. These values are considerably smaller than the estimated trap depth from V_{SC} measurements, being 0.3−0.5 eV in the same light intensity range. The effective trap depth can also be estimated from charge extraction measurements, using eq 3. Figure 4 shows the calculated variation of the Fermi-level in the nanostructured TiO_2 film under short-circuit conditions. It is evident that the Fermi-level is practically constant in most of the film, decreasing sharply in about 1 μm adjacent to the conducting substrate. In this first micrometer, it is likely that the conduction band electrons are not in thermal equilibrium with the trap states.[15] The measured activation energy for charge transport will therefore be determined by $(E_C - E_F)$ in the bulk of the film. From Figure 4, it follows that the effective trap depth, corresponding to $E_a(\tau_{IMPS})$, is about 0.4 eV if the diffusion coefficient for electrons in the TiO_2 conduction band is taken as 0.5 cm^2 s^{-1} (single-crystal value). Alternatively, we calculated a value of ~0.24 eV for a 1000 times smaller diffusion coefficient, as the diffusion coefficient is expected to be reduced due to scattering electrons at grain boundaries. The calculated activation energy values differ significantly from the experimental values.

We can also use the measured activation energy as a starting point for a comparison with the trapping/detrapping model. The measured $E_a(\tau_{IMPS})$ value will correspond to the effective trap depth $(E_C - E_T)$, which is approximately equal to $(E_C - E_F)$ at that specific light intensity.[10] The density of conduction band electrons (n_C) can be calculated using eq 5

$$n_C = N_C \exp\left(-\frac{E_C - E_F}{kT}\right) \tag{5}$$

where N_C is the effective density of conduction band states and kT the thermal energy. Assuming N_C to be 10^{20} cm^{-3}, corresponding to an effective electron mass m^* in anatase TiO_2 of $2.5m_e$, n_C is calculated to be 2×10^{18} cm^{-3} for $(E_C - E_F) = 0.1$ eV. This corresponds to an electronic charge in the conduction band of 2×10^{-4} C cm^{-2} for the 12 μm nanostructured TiO_2 electrode (taking the porosity of the TiO_2 film of 0.5 into account). Comparison with Table 1 shows that this value is about 3 times higher than the total extracted charge found experimentally. If the effective density of trap states $N_{T,eff}$ is similar

to N_C, the total (free and trapped) electron charge will be about 10 mC cm^{-2}, as follows from a Boltzmann distribution between trapped and free electrons (eq 6)

$$\frac{n_C}{n_T} = \frac{N_C}{N_{T,eff}} \exp\left(-\frac{E_C - E_T}{kT}\right) \quad (6)$$

The large discrepancy between the calculated charge and the experimentally determined value appears to be in conflict with the trapping/detrapping model, although one could argue about the accuracy of the N_C and $N_{T,eff}$ values. A reasonable fit with the experimental charge can, for instance, be obtained if $N_C = 10^{19}$ cm^{-3} ($m^* = 0.6m_e$) and $N_{T,eff} = 4 \times 10^{17}$ cm^{-3}. About 30% of the electrons are then, however, free in the conduction band, which opposes the argument for the trapping/detrapping model (i.e., that only a very small fraction of the total number of electrons is free, thereby causing the low effective diffusion coefficient).

Toward Alternative Models.

The experimental findings in this study are not easy to unite with the trapping/detrapping model for electron transport in nanostructured TiO_2. One should therefore consider the possibility that the trapping/detrapping mechanism, although useful as a model, does not reflect the actual situation in the nanostructured TiO_2 solar cell. Several aspects of this cell definitely need further attention. Here we list some of them.

Separate Nanocrystals.

The nanostructured electrode consists of separate TiO_2 particles. Each particle tends to be single crystal. The nanocrystals are, however, connected in a random way to each other. The particle−particle connection will most likely be a distinct grain boundary, where the material properties differ from those in the bulk of the nanocrystal. Electrons can probably move freely within a nanocrystal but experience some kind of barrier to move to an adjacent nanocrystal. The limiting step for electron transport could therefore be the jump from one nanocrystal to the next. To model the mesoporous nanocrystal film as a homogeneous medium would probably be an oversimplification. The nanocrystals should probably be treated as separate units instead.

Electron Repulsion.

This study has shown that several electrons can accumulate in a single TiO_2 nanocrystal under normal solar cell operation conditions. Electrostatic repulsion between these electrons should therefore be taken into account. Because of the high dielectric constant of anatase TiO_2 the repulsion energy will be modest,[11] but it is estimated to be larger than kT when more than four electrons are accumulated per particle.

Unpinning of the Band Edges.

The charge of the electrons that are accumulated in TiO_2 will result in a certain band edge shift due to unpinning of the band edges. The value of the Helmholtz capacitance (C_H) of the TiO_2/dye/organic electrolyte interface is unknown, but it is probably smaller than the C_H of pure TiO_2 in aqueous solutions ($\sim 10^{-5}$ F cm^{-2}). If $C_H = 10^{-6}$ F cm^{-2}, E_C would increase 8 meV with every additional electron per TiO_2 nanocrystal. It might also be possible that accumulation of electrons in TiO_2 leads to additional adsorption of cations at the semiconductor/electrolyte interface. Band edge shifts will then be avoided, but the electrostatic attraction by the fixed positive charge could affect electron transport.

Conclusions

The electron transport in mesoporous nanocrystalline TiO_2 in dye-sensitized solar cells is a thermally activated process with activation energies in the range of 0.10−0.15 eV. These values appear to be conflicting with the generally accepted trapping/detrapping model with an exponential distribution of traps, where larger activation energies are expected. Using a novel experimental technique, it is demonstrated that there is a large gradient in the electrochemical potential inside the nanostructured TiO_2 film when the solar cell is operated under short-circuit conditions.

Acknowledgment. This work was financed by the Swedish Energy Agency, the Swedish Foundation for Strategic Environmental Research, and PSO Project 3629 (Denmark). We thank Dr. Leif Häggman for solar cell preparation and Dr. Michael Wang for technical assistance.

References and Notes

(1) O'Regan, B.; Grätzel, M. *Nature* **1991**, *353*, 737−740.
(2) Hagfeldt, A.; Grätzel, M. *Acc. Chem. Res.* **2000**, *33*, 269−277.
(3) Bisquert, J.; Cahen, D.; Hodes, G.; Ruehle, S.; Zaban, A. *J. Phys. Chem. B* **2004**, *108*, 8108−8118.
(4) Cao, F.; Oskam, G.; Searson, P. C. *J. Phys. Chem.* **1996**, *100*, 17021−17027.
(5) Dloczik, L.; Ileperuma, O.; Lauermann, I.; Peter, L.; Ponomarev, E.; Redmond, G.; Shaw, N.; Uhlendorf, I. *J. Phys. Chem. B* **1997**, *101*, 10281−10289.
(6) Solbrand, A.; Henningsson, A.; Södergren, S.; Lindström, H.; Hagfeldt, A.; Lindquist., S.-E. *J. Phys. Chem. B* **1999**, *103*, 1078−1083.
(7) Schlichthörl, G.; Park, N. G.; Frank, A. J. *J. Phys. Chem. B* **1999**, *103*, 782−791.
(8) van de Lagemaat, J.; Frank, A. J. *J. Phys. Chem. B* **2000**, *104*, 4292−4294.
(9) Kopidakis, N.; Schiff, E. A.; Park, N.-G.; van de Lagemaat, J.; Frank, A. J. *J. Phys. Chem. B* **2000**, *104*, 3930−3936.
(10) Fisher, A. C.; Peter, L. M.; Ponomarev, E. A.; Walker, A. B.; Wijayantha, K. G. U. *J. Phys. Chem. B* **2000**, *104*, 949−958.
(11) van der Zanden, B.; Goossens, A. *J. Phys. Chem. B* **2000**, *104*, 7171−7178.
(12) Nakade, S.; Saito, Y.; Kubo, W.; Kitamura, T.; Wada, Y.; Yanagida, S. *J. Phys. Chem. B* **2003**, *107*, 8607−8611.
(13) Nakade, S.; Kubo, W.; Saito, Y.; Kanzaki, T.; Kitamura, T.; Wada, Y.; Yanagida, S. *J. Phys. Chem. B* **2003**, *107*, 14244−14248.
(14) Goossens, A.; van der Zanden, B.; Schoonman, J. *Chem. Phys. Lett.* **2000**, *331*, 1−6.
(15) van de Lagemaat, J.; Frank, A. J. *J. Phys. Chem. B* **2001**, *105*, 11194−11205.
(16) Schlichthörl, G.; Huang, S. Y.; Sprague, J.; Frank, A. J. *J. Phys. Chem. B* **1997**, *101*, 8139−8153.
(17) Boschloo, G.; Hagfeldt, A. *Chem. Phys. Lett.* **2003**, *370*, 381−386.
(18) Södergren, S.; Hagfeldt, A.; Olsson, J.; Lindquist, S. E. *J. Phys. Chem.* **1994**, *98*, 5552−5556.
(19) Vanmaekelbergh, D.; de Jongh, P. E. *J. Phys. Chem. B* **1999**, *103*, 747−750.
(20) Greijer-Agrell, H.; Boschloo, G.; Hagfeldt, A. *J. Phys. Chem. B* **2004**, *108*, 12388−12396.
(21) Forro, L.; Chauvet, O.; Emin, D.; Zuppiroli, L.; Berger, H.; Lévy, F. *J. Appl. Phys.* **1994**, *75*, 633−635.
(22) de Jongh, P. E.; Vanmaekelbergh, D. *Phys. Rev. Lett.* **1996**, *77*, 3427−3430.
(23) Lindström, H.; Magnusson, E.; Holmberg, A.; Södergren, S.; Lindquist, S.-E.; Hagfeldt, A. *Sol. Energy Mater. Sol. Cells* **2002**, *73*, 91−101.
(24) Duffy, N. W.; Peter, L. M.; Rajapakse, R. M. G.; Wijayantha, K. G. U. *J. Phys. Chem. B* **2000**, *104*, 8916−8919.
(25) Peter, L. M.; Duffy, N. W.; Wang, R. L.; Wijayantha, K. G. U. *J. Electroanal. Chem.* **2002**, *524*, 127−136.
(26) Zaban, A.; Greenshtein, M.; Bisquert, J. *ChemPhysChem* **2003**, *4*, 859−864.
(27) Fabregat-Santiago, F.; Mora-Sero, I.; Garcia-Belmonte, G.; Bisquert, J. *J. Phys. Chem. B* **2003**, 758−768.
(28) Montanari, I.; Nelson, J.; Durrant, J. R. *J. Phys. Chem. B* **2002**, *106*, 12203−12210.
(29) Bauer, C.; Boschloo, G.; Mukhtar, E.; Hagfeldt, A. *J. Phys. Chem. B* **2002**, *106*, 12693−12704.
(30) Bisquert, J.; Zaban, A.; Greenshtein, M.; Mora-Sero, I. *J. Am. Chem. Soc.* **2004**, *126*, 13550−13559.